

EVIDENCE FOR $\pi^+\pi^-$ RESONANCES AT 395- AND 520-MeV EFFECTIVE MASS*

N. P. Samios

Brookhaven National Laboratory, Upton, New York

and

A. H. Bachman and R. M. Lea

The City College of New York, New York, New York

and

T. E. Kalogeropoulos

Columbia University, New York, New York

and

W. D. Shephard

University of Kentucky, Lexington, Kentucky

(Received June 21, 1962)

The purpose of this Letter is to present evidence of two heretofore unreported resonances which occur in the $(\pi^+\pi^-)$ state with effective masses of 395 MeV and 520 MeV. The ρ and N_{33}^* were also observed,¹ the ρ appearing as a single peak with $m_\rho = 740$ MeV and the isobar N_{33}^* with $m_{33} = 1220$ MeV.

The resonances were observed in a study of 1240 four-prong events obtained by exposing the BNL 20-in. liquid hydrogen bubble chamber to a 4.7-BeV/c π^- beam at the AGS. The exposure consisted of about 20 000 good quality pictures with approximately 20 tracks per picture. The events selected for measurement satisfied the following criteria: They occurred in a restricted fiducial volume; they had no tracks less than 5 cm in length; and they had no two tracks less than 10 cm in length. These criteria assured reasonably good effective mass measurements. The events were analyzed using the BNL TRED-STEER programs. The production hypotheses considered for each event were

- I. $\pi^- + p \rightarrow 2\pi^- \pi^+ p$,
- IIa. $\rightarrow 2\pi^- \pi^+ p \pi^0$,
- IIb. $\rightarrow 2\pi^- \pi^+ p$ (neutrals),
- IIIa. $\rightarrow 2\pi^- 2\pi^+ n$,
- IIIb. $\rightarrow 2\pi^- 2\pi^+$ (neutrals).

The following criteria were adopted in determining whether an event fit one of the above hypotheses: Its χ^2 probability for the given hypothesis must have been greater than 2%, and the visual estimates of bubble density must have agreed with that predicted by the assumed hypothesis. In the latter respect, a 1.5 \times minimum track could def-

initely be distinguished from one of 1.0 \times minimum. In the case of plural fits the event was classified as ambiguous unless the χ^2 probability differed by a factor of 5. The ambiguous events will be discussed below. Table I contains a listing of the number of events in each channel.

The (π^+p) and $(\pi^+\pi^-)$ effective mass distributions for the 240 events which were classified as Reaction I are shown in Figs. 1(a) and (b). The results presented in Fig. 1 also include 24 ambiguous events which were consistent with both Reactions I and IIa. Since substantially all of these ambiguous events had a higher χ^2 probability for the four-constraint Reaction I than for the one-constraint Reaction IIa, and since their numerical weight is small, they were included in that figure.

The ρ and N_{33}^* isobar resonances clearly dominate Reaction I. In order to investigate the structure of these resonant peaks, the invariant phase-space distribution normalized to the events with effective mass greater than 1400 MeV and greater than 1100 MeV, respectively, were included in Figs. 1(a) and (b). For the purpose of the following treatment, it was assumed that there were no interference effects and that the phase space normalized in this manner was a good representation of the background. This background was then subtracted from the histograms in Figs. 1(a) and (b). The results are presented in Figs. 1(c) and (d), respectively. The masses and widths of the resonances obtained from these plots are shown in Table II. It is clear that the widths obtained by this procedure are sensitive to what is defined as background. The agreement, however, of the properties of the N_{33}^* with the known value and width of this isobar supports the

Table I. Tabulation of number events and pion combination for each reaction.

Event type	Number of events	Number of $\pi^+\pi^-$ combinations	Number of $\pi^\pm\pi^\pm$ combinations
I ($\pi^-\pi^-\pi^+\rho$)	240		
Ambiguous I	<u>24</u>		
	264	528	
IIa ($\pi^-\pi^-\pi^+\rho\pi^0$)	345		
IIb ($\pi^-\pi^-\pi^+\rho$ + neutrals)	<u>121</u>		
	466	932	466
IIIa ($\pi^-\pi^-\pi^+\pi^+n$)	168		
Ambiguous IIIa	38		
IIIb ($\pi^-\pi^-\pi^+\pi^+$ + neutrals)	201		
Ambiguous IIIb	<u>85</u>		
	510	2040	1020
Totals IIa, b, IIIa, b	976	2972	1486

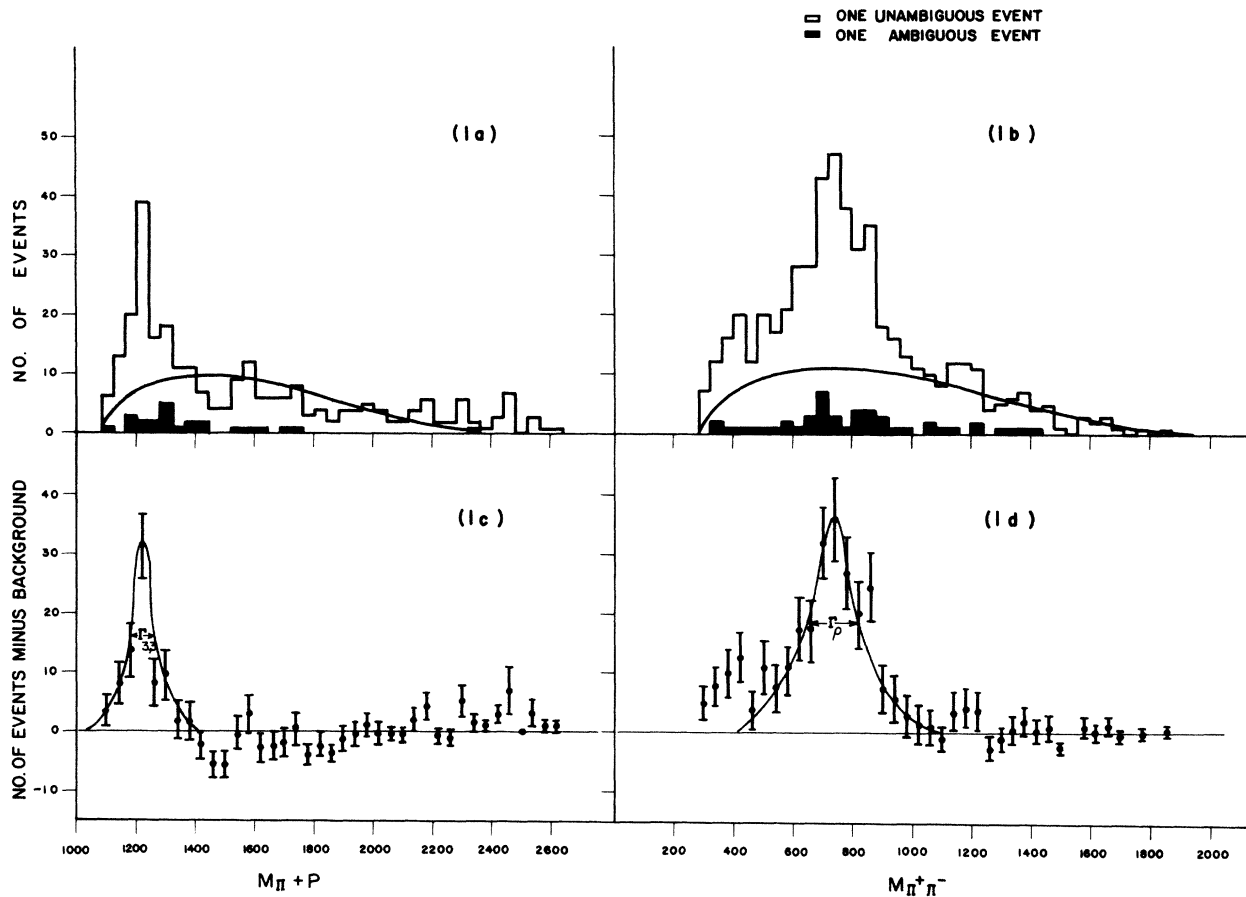


FIG. 1. (a) Histogram of the effective-mass distribution for the 264 ($\pi^+\rho$) combinations from Reaction I. (b) Histogram of the effective-mass distribution for the 528 ($\pi^+\pi^-$) combinations from Reaction I. The smooth curves are invariant phase-space distributions normalized to the events with mass >1400 MeV and >1000 MeV, respectively. (c), (d) The distributions in (a) and (b), respectively, with the smooth curve subtracted. The errors shown are \sqrt{N} , where N is the total number of pion pairs per 40-MeV interval before subtraction.

Table II. Tabulation of the properties of the observed resonances.

Resonance	Effective mass (MeV)	Full width at half max. (MeV)	Reactions	Number of events	Number of events in each resonance
N_{33}^*	1220 ± 20	90 ± 20	$2\pi^- \pi^+ p$	264	~ 75
ρ^0	740 ± 30	170 ± 30			~ 225
$(\pi^+ \pi^-)_1$	395 ± 10	50 ± 20	All reactions except $2\pi^- \pi^+ p$	976	~ 173
$(\pi^+ \pi^-)_2$	520 ± 20	70 ± 30			~ 176
ρ^0	750 ± 20	150 ± 20			~ 190

adopted procedure. The data, within statistics, are consistent with a single ρ resonance. Furthermore, some excess of events above background is noted in the region of 400-MeV ($\pi^+ \pi^-$) effective mass.

From Figs. 1(c) and (d) it is estimated that there are ~ 75 ($\pi^+ p$) isobars and ~ 225 ρ 's in the 264 events of Reaction I. These numbers should be considered only as approximate since they are strongly dependent on the knowledge of the background. However, it is clear that this reaction proceeds via two intermediate states, namely, $\pi^- p \rho$ and $\pi^- N_{33}^* \pi^-$.

The evidence for two additional ($\pi^+ \pi^-$) resonances is obtained from the 976 events which involve the production of one or more neutral

particles, i.e., event types IIa,b and IIIa,b. Table I shows that this group of events represents about 80% of the four-prong events studied. The ambiguous IIIa and ambiguous IIIb types referred to in Table I include events which were compatible with both Reaction IIa and IIIa, and Reaction IIb and IIIb, respectively. In view of the greater probability that these ambiguous events are of type III they have been included in the results which follow with that classification.²

The ($\pi^\pm \pi^\pm$) and ($\pi^+ \pi^-$) effective mass distributions for the 1486 like combinations and the 2972 unlike combinations are shown in Figs. 2(a) and 3(a), respectively. Measured values of track momenta and angles were used in calculating the effective masses.³ The like pion distribution

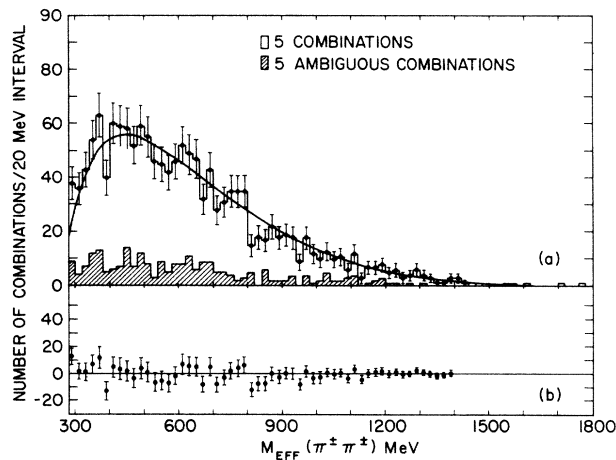


FIG. 2. (a) Histogram of the effective-mass distribution for the 1486 ($\pi^+ \pi^+ \pi^+$) combinations from Reactions IIa,b and IIIa,b. The smooth curve is the invariant phase-space distribution normalized to the total number of events. (b) The distribution in (a) with the smooth curve subtracted. The errors shown are \sqrt{N} , where N is the total number of pion pairs per 20-MeV interval before subtraction.

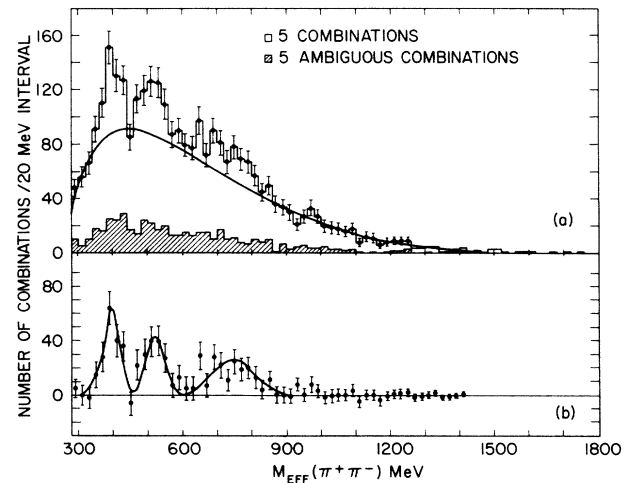


FIG. 3. (a) Histogram of the effective-mass distribution for the 2972 ($\pi^+ \pi^-$) combinations from Reactions IIa,b and IIIa,b. The smooth curve is the invariant phase-space distribution normalized to the events with mass > 850 MeV. (b) The distribution in (a) with the smooth curve subtracted. The errors shown are \sqrt{N} , where N is the total number of pion pairs per 20-MeV interval before subtraction.

shows no significant peaking and can be fitted by an invariant phase-space distribution composed of five-, six-, and seven-body final states. The amount of each final-state contribution is approximately equal to the amount of production in each of these channels. This distribution, based on phase space, is shown by the solid curve in Fig. 2(a). The agreement of the phase-space distribution with the experimental distribution is indicated in Fig. 2(b), which shows the difference of the two distributions.

On the other hand, the effective-mass distribution of the unlike pions, shown in Fig. 3(a), exhibits definite structure in the region of low mass values.⁴ It is impossible to draw a smooth curve, based on phase space, that is consistent with the data in the region between 360- and 560-MeV effective mass. This is due, mainly, to the valley that exists at 450 MeV. The experimental resolution in this region of effective mass, as obtained from the variance-covariance matrix calculated by the IBM-7090 GUTS program, is ± 5 MeV. This value for the resolution was confirmed by the results of $(\pi^+\pi^-)$ effective mass measurements made on 47 known $K_1^0 \rightarrow \pi^+\pi^-$ events which were observed in the same exposure.

In order to determine the structure in the unlike-pion effective-mass distribution, the procedure followed was similar to that which gave consistent results in the case of Reaction I. The background for like- and unlike-pion combinations was assumed to be the same. This background distribution was then normalized to the events with effective mass greater than 850 MeV. The resulting curve is shown in Fig. 3(a). Figure 3(b) shows the experimental distribution with the background subtracted. This difference curve shows three resonances with the following masses and widths in MeV:

$$m_1 = 395 \pm 10, \Gamma_1 = 50 \pm 20;$$

$$m_2 = 520 \pm 20, \Gamma_2 = 70 \pm 30;$$

$$m_\rho = 750 \pm 20, \Gamma_\rho = 150 \pm 20.$$

The first two are previously unreported resonances. The third is in good agreement with the previously observed ρ . Estimates of the number of events in each peak are presented in Table II. A separate examination of the results for Reaction II and for Reaction III indicates that the

major contributions to the m_1 and m_2 effects discussed above come from the events in which the nucleon is a neutron, i.e., Reaction III.

A search was also made for these new resonances in a singly charged state in the 345 events of type IIa. The effective-mass distribution for $(\pi^\pm\pi^0)$ combinations in these events shows evidence of the ρ as well as a peak above invariant phase space in the region around 500-MeV effective mass. However, due to the limited statistics and the poorer experimental resolution obtained with combinations involving a neutral pion, it is difficult to determine whether there is any correspondence between this deviation from phase space and the previously discussed m_1 and m_2 resonances in the $(\pi^+\pi^-)$ state. Therefore, the isotopic spin of these two new resonances can be either 0 or 1 but not 2.

We wish to thank the AGS staff and the operating crew of the BNL bubble chamber for aid in obtaining these pictures. We also wish to thank T. W. Morris for the use of his STEER program.

*Work performed under the auspices of the U. S. Atomic Energy Commission. Research supported in part by the National Science Foundation.

¹For a list of references of previously observed two-pion resonances see, for example, B. Sechi Zorn, Phys. Rev. Letters **8**, 282 (1962). In addition, J. Schwartz, J. Kirz, and R. Tripp, Bull. Am. Phys. Soc. **7**, 282 (1962) have reported an enhancement for $(\pi^+\pi^-)$ effective mass >340 MeV.

²In each of these ambiguous events only one of the positive tracks was definitely identified as a pion by reason of its observed density. The other positive track had a momentum greater than 1.3 BeV/c and, hence, was not identifiable by density observation. Considerations based on the observed number of definite and ambiguous events of types II and III and the observed momentum spectra of positive pions and protons indicate that more than 80% of the above-mentioned ambiguous events should be classified as Reactions IIIa, b. Further, it should be noted that the cross-hatched area of the effective-mass histogram in Fig. 3 representing the ambiguous events is of relatively small numerical weight and exhibits no special structure.

³Effective-mass distributions using fitted values of track momenta and angles were obtained for the reactions involving only one neutral particle, IIa and IIIa. These distributions were similar in structure to those obtained using measured values.

⁴For example, the χ^2 probability of the $\pi^\pm\pi^\pm$ data fitting the phase-space curve in Fig. 2(a), evaluated for all intervals, is 0.30. The same probability for the $\pi^+\pi^-$ data is less than 0.0001.